On the Influence of the Morphological Structure on the Liquid Crystalline Behavior of Liquid Crystalline Side Chain Block Copolymers

H. Fischer,*,† S. Poser,‡ M. Arnold,‡ and W. Frank‡

H. H. Wills Physics Laboratory, University of Bristol, Tyndall Avenue, Royal Fort, Bristol BS8 1TL, U.K., and Institute for Technical Chemistry, Martin-Luther University Halle-Wittenberg, Neuwerk 7, Halle-Saale 06108, F.R.G.

Received February 10, 1994; Revised Manuscript Received July 7, 1994•

ABSTRACT: The influence of the morphological structure on the phase behavior of a liquid crystalline side chain block copolymer has been investigated using SAXS, DSC, TEM, and low-angle electron diffraction. All samples of poly[styrene-*block*-2-((3-cholesteryloxycarbonyl)oxy)ethyl methacrylate] (PS-*b*-PChEMA) show a phase separation between the two blocks. An influence on the phase structure of the liquid crystalline subphase exerted by the morphological structure was observed. It was found that in the case of those samples where the liquid crystalline subphase is not continuous (spheres), only a nematic phase is seen, whereas in all samples in which there is a continuous liquid crystalline subphase, the smectic A phase of the homopolymer is formed.

Introduction

Block copolymers are an interesting and already well-studied variation of polymers. In this class of polymers it is possible to combine the properties of two completely different polymers with no macroscopic phase separation occurring. Owing to the chemical link between the noncompatible polymers, the phase separation is limited to a microscopic scale and is dependent on the volume fraction of the different blocks. Several different morphological structures have been predicted and observed. These morphologies are spheres in a cubic lattice, rods in a hexagonal lattice embedded in the matrix of the other component of the block copolymers, or lamellae of both. Recently, ordered bicontinuous morphologies were also found.[1-5] These double-diamond structures, space group *Pn*3*m* (OBDD), were found for volume fractions in between the lamellar and the rodlike hexagonal phase. So the scheme for the morphologies of the block copolymers is, as described by Bates and Fredrickson,[6] a sequence of spherical, rodlike hexagonal, double diamond, and lamellar phases.

If one of the blocks is a liquid crystalline (LC) side group polymer, two different scales of phase separation might be obtained. It is now the aim to study the influence of the morphology of the block copolymer on the phase structure of the LC block. It is extremely important for these studies to have a narrow molecular weight distribution of the synthesized substances to get a clear phase separation and a narrow interfacial area. The best way to obtain this is with a living anionic polymerization. However, it is very difficult to find a comonomer with a mesogenic group attached which is stable against the attack of the strong anions present during the chain growth reaction.[7-10] Therefore, polymer-analogous reactions on preformed block copolymers were performed to obtain the block copolymer with a LC block.[11-13] Initial investigations on poly[styrene-*block*-2-((3-cholesteryloxycarbonyl)oxy)ethyl methacrylate]s (PS-*b*-PChEMA) and poly[butadiene-*block*-2-((3-cholesteryloxycarbonyl)oxy)-ethyl methacrylate]s (PB-*b*-PChEMA) suggested an influence of the amorphous block on the phase structure of the LC block which was dependent on the type of monomer in the A block for a lamellar structure.[12] More systematic investigations have been carried out now using di- and triblock copolymers of poly[styrene-*block*-2-((3-cholesteryloxycarbonyl)oxy)ethyl methacrylate]s (PS-*b*-PChEMA[13] and PChEMA-*b*-PS-*b*-PChEMA) (see Figure 1) to determine the influence of the different block lengths and thus the change in the morphology on the phase behavior of the LC phase.

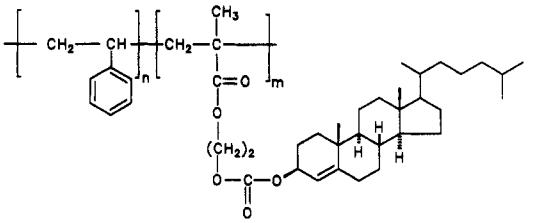

Figure 1. Chemical structure of the block copolymers.

Experimental Section

The block copolymers were synthesized and characterized as described previously.[12,13] Lithium naphthalene, instead of *sec*-butyllithium, was used as an initiator for the first step of the anionic polymerization of styrene to obtain the triblock copolymers. Samples for transmission electron microscopy (TEM) and differential scanning calorimetry (DSC) were prepared by casting ~1 mm thick films from dilute solutions of the polymers in toluene over a period of about 10 days at 25 °C and annealing them afterward at 130 °C for 24 h under vacuum. The samples were cut using a diamond knife at room temperature, and the thin films (~10 nm thick) were transferred onto copper grids. To get sufficient contrast for TEM and low-angle electron diffraction studies,[14,15] the styrene parts of the samples were stained with RuO_4 vapor at 25 °C for about 30 min.[16] Alternatively, the methacrylate parts were stained with OsO_4 after the reaction of the methacryl ester group with hydrazine using the technique described by Kanig and Misra.[18,19] For the TEM studies and the low-angle electron diffraction experiments, a Philips EM 301 was used. The diffraction experiments were performed as described elsewhere.[15,19] DSC traces were obtained using a Perkin-Elmer DSC 7 with heating and cooling rates of 10 K/min. Optical microscopy (POM) was performed using a Zeiss Ultraphot combined with a Linkam HM 600 hot stage and

† University of Bristol. Currently: TUE Eindhoven, Vac. Scheih. Techn., Postbus 513, 5600 MB Eindhoven, The Netherlands.
‡ Martin-Luther University Halle-Wittenberg.
• Abstract published in *Advance ACS Abstracts*, October 1, 1994.

0024-9297/94/2227-7133$04.50/0

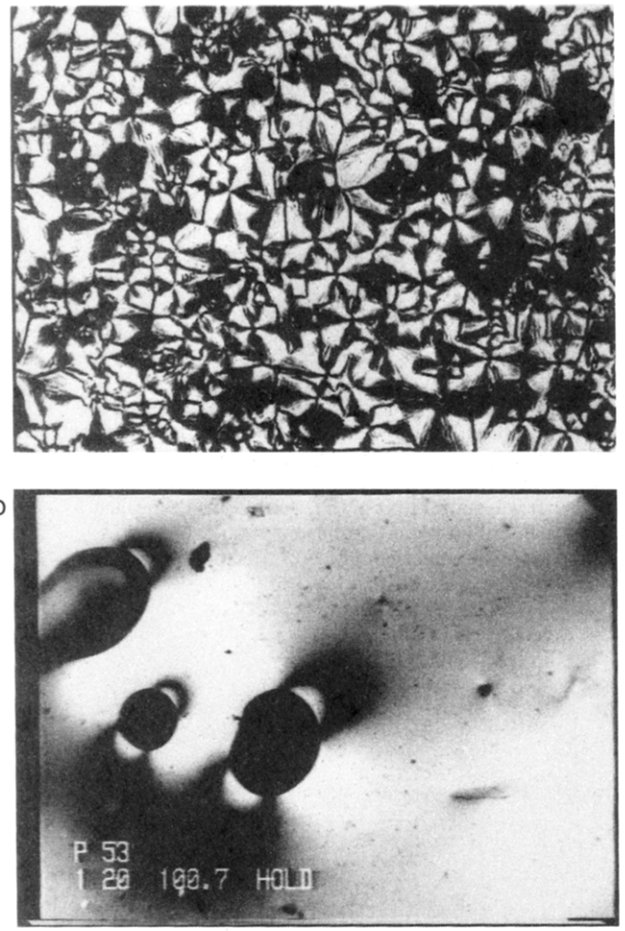

Figure 2. Optical micrographs of (a) sample 78 (fan-shaped texture of a smectic A phase), and (b) sample 53 (nematic texture, crossed polarizers).

a Sony video recorder. X-ray studies were carried out using an Eliott GX 21 with a copper target combined with a Siemens X-1000 area detector and a Rigaku Denki small-angle film camera. More precise small-angle measurements were performed at the synchrotron facility in Daresbury, England, beamline 8.2, with a camera length of 3.5 m.

Results and Discussion

The investigated block copolymers were characterized as described in ref 13 using GPC, DSC, and POM. As with the LC homopolymer (PChEMA), liquid crystalline behavior was observed for most of the block copolymers synthesized, as shown by DSC measurements and polarization microscopic investigations (see Figure 2, Table 1). Parts a and b of Figure 2 show the typical textures found. X-ray measurements confirmed the existence of a smectic A phase for these samples (see Figure 3). The layer spacing was found to be 45 Å (inner reflection), and the lateral distance between the mesogens of 5.5 Å is in good agreement with the values found for cholesteryl derivatives. The smectic phase was identified to be a smectic A since no tilt of the layer reflections with respect to the wide-angle reflection and only one diffuse wide-angle reflection (unordered structure) were observed. The copolymer samples with the shortest LC blocks are exceptions to this. They were found to form a nematic phase with an isotropization temperature as determined in the polarizing microscope only, since there was no evidence of a liquid crystalline phase from the DSC measurements and X-ray diffraction. For these samples only diffuse layer reflections were observed. The POM pictures 2a and 2b show instead a difference in textures for the different liquid crystalline

Table 1. Molecular Weight, Molecular Weight Distribution, and Thermal Data of the Synthesized Block Copolymers[a]

sample	M_n (PS)	M_n (copolymer)	Φ_{PS}	D	phase behavior (°C)
PS			1.00		g 102 i
Diblock Copolymers PS-*b*-PChEMA					
53	57500	73200	0.78	1.07	g 105 g 126 n 188 i
55	48300	71000	0.67	1.07	g 101 g 126 S_A 187 i
57	62200	109000	0.56	1.11	g 103 S_A 197 i
59	51000	133000	0.37	1.11	g 103 g 126 S_A 202 i
78	20400	64000	0.30	1.03	g 91 g 120 S_A 189 i
82	18400	111000	0.16	1.11	g 100 g 127 S_A 200 i
75	10100	63000	0.15	1.18	g 91 g 123 S_A 198 i
61	25000	202000	0.11	1.10	g 102 g 125 S_A 199 i
Triblock Copolymers PChEMA-*b*-PS-*b*-PChEMA					
DB2	29100	54300	0.53	1.15	g 100 g 119 S_A 190 i
DB4	22200	77300	0.29	1.15	g 101 g 117 S_A 184 i
DB7	25600	75000	0.33	1.20	g 102 g 118 S_A 199 i
DB5	22600	64000	0.35	1.15	g 98 g 118 S_A 186 i
DB6	24000	43000	0.55	1.20	g 101 g 118 S_A 183 i
DB8	21000	29000	0.70	1.05	g 98 g 118 n 193 i
DB9	26000	29000	0.88	1.04	g 98 g n 194 i
DB10	20000	87000	0.22	1.47	g 103 g 118 S_A 201 i
DB11	34000	57000	0.59	1.25	g 99 g 120 S_A 194 i
DB12	52000	78000	0.66	1.12	g 95 g 119 S_A 180 i
DB14	26000	45000	0.57	1.13	g 93 g 118 S_A 197 i
DB15	37700	53500	0.70	1.09	g 103 g 116 S_A 200 i
DB16	54400	68000	0.77	1.09	g 93 g n 194 i
DB17	21000	23000	0.90	1.10	g 98 g n 184 i
DB18	37000	42000	0.88	1.26	g 92 g n 195 i
DB19	51200	53000	0.96	1.08	g 98 g i
DB20	22700	26700	0.84	1.06	g 96 g n 186 i
DB21	34700	37000	0.93	1.07	g 98 g n 194 i
PChEMA		250000	0.00	1.90	g 126 S_A 213 i

[a] $D \equiv$ polydispersity; $\Phi_{PS} \equiv$ volume fraction of PS, calculated using the densities for PS (ρ = 1.02 g/cm^3) and PChEMA (ρ = 0.99 g/cm^3).

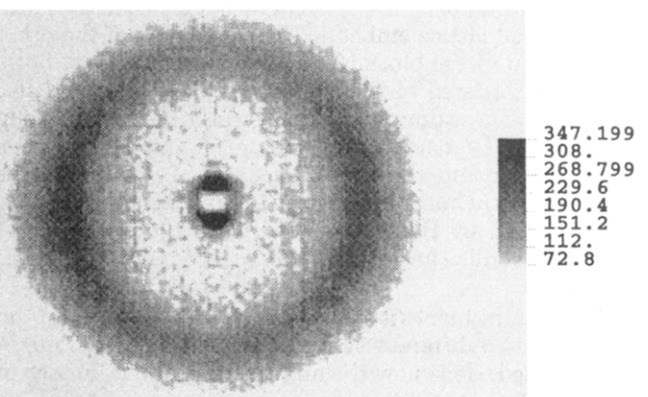

Figure 3. X-ray diffraction pattern of the smectic A phase of sample 78 (oriented fiber, 25 °C).

phases. The fan-shaped texture in Figure 2a is typical for a smectic A phase whereas the texture shown in Figure 2b hints to a nematic phase.

DSC measurements of annealed samples show, in general, two glass transition temperatures (see Figure 4). The separation of the glass transitions in the block copolymer can only be explained by a phase separation of the two different blocks. The two glass transition temperatures, therefore, correspond to the glass transition temperatures of the homopolymers of block A (PS) and those of block B (PChEMA). Both glass transitions are labeled in Figure 4 since especially the glass transition of PChEMA has only a small heat capacity (0.05 J g^{-1} K^{-1}). Additional to the two glass transitions it is possible to observe a peak corresponding to the transformation of the mesophase into an isotropic melt. A plot of the transition enthalpies at the temperature where the mesophase

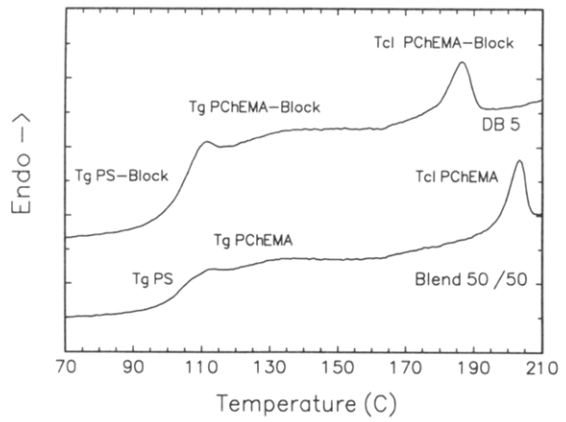

Figure 4. DSC traces of the triblock copolymer DB5 and of a mixture of both homopolymers with volume contents of 50%, respectively (10 K/min, second heating scan).

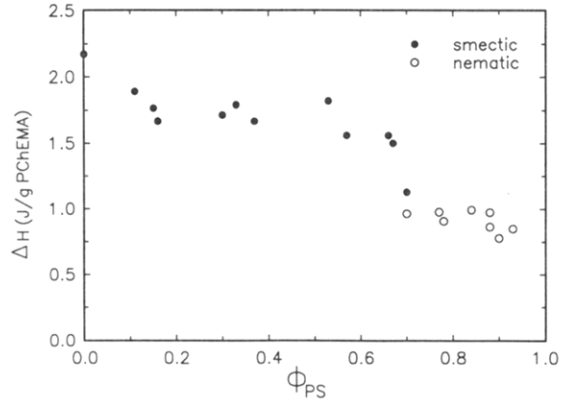

Figure 5. Plot of the transition enthalpies of the block copolymers at the clearing point vs Φ_{PS}.

transforms into an isotropic melt (clearing points) versus the volume fraction of polystyrene, Φ_{PS}, is shown in Figure 5. The transition enthalpy is scaled to the absolute amount of LC polymer. The drop in transition enthalpy of the smectic phases from the homopolymer to the copolymer can be explained by the existence of the interface region between the two separated polymers. The nematic phases show a smaller heat of transition at the clearing point owing to their lower order. However, a distinct difference in value is noticeable for the block copolymers displaying a smectic A phase and for those showing a nematic phase.

The phase separation of the two blocks could be confirmed by small-angle X-ray diffraction studies of unoriented samples (see Figure 6, Table 2). Besides the reflection at 45 Å indicating a smectic order in the liquid crystalline subphase, more intense reflections at ~200 Å were observed. These reflections arise from the electron

Table 2. Morphological Data of the Observed Block Copolymers

		SAXS (Å)		
sample	Φ_{PS}	layer reflection	reflection from block separation	morphology (TEM)
PS	1.00			
		Diblock Copolymers PS-*b*-PChEMA		
53	0.78	(45)	392, 192	PChEMA spheres
55	0.67	45	420	lamellae
57	0.56	45	440, 220, 147	lamellae
59	0.37	45	510, 267, 245	PS cylinders
78	0.30	45	393, 227	PS spheres
82	0.16	45	340, 240, 200	PS spheres
75	0.15	45	187	PS spheres
61	0.11	45	324, 165	PS spheres
		Triblock Copolymers PChEMA-*b*-PS-*b*-PChEMA		
DB2	0.53	45	230, 116, 77	lamellae
DB4	0.29	45	200, 160, 105	PS cylinders
DB5	0.35	45	196, 157	PS cylinders
DB6	0.55	45	180	lamellae
DB7	0.33	(45)	214, 102, 77	PS cylinders
DB8	0.70	(45)	170	PChEMA spheres
DB9	0.88	45	163	PChEMA spheres
DB10	0.22	45	185	PS spheres
DB11	0.59	45	250, 125	lamellae
DB12	0.66	45	255, 132	lamellae
DB14	0.57	45	180, 90	lamellae
DB15	0.70	(45)	224, 112	lamellae
DB16	0.77	(45)	280	PChEMA spheres
DB17	0.90		140	PChEMA spheres
DB18	0.88	(45)	150	PChEMA spheres
DB19	0.96		130	PChEMA spheres
DB20	0.84	(45)		PChEMA spheres
DB21	0.93			PChEMA spheres
PChEMA	0.00	45		

density differences between the two separated copolymer blocks. An investigation of the morphology formed after phase separation was possible by examining further reflections than the first and strongest SAXS reflection. Figure 7 shows the observed reflection for sample DB2. The reflections could be indexed as 001, 002, and 003 and attributed to a lamellar morphology (Table 2). In principle, the expected morphologies were found and vary with the volume ratios of the different blocks in the copolymers. A direct investigation of the present morphology of the phase-separated block copolymers was possible by TEM of thin films of the block copolymers. To increase the contrast between the two blocks, it was necessary to stain the polystyrene block using RuO_4 vapor.[16] Figures 8–11 show representative pictures of the observed morphology. At first, a blend of the two homopolymers was examined to show that macroscopic phase separation (Figure 8) occurs. As can be seen in the other figures, lamellar (Figure 10a,b), cylindrical (Figure

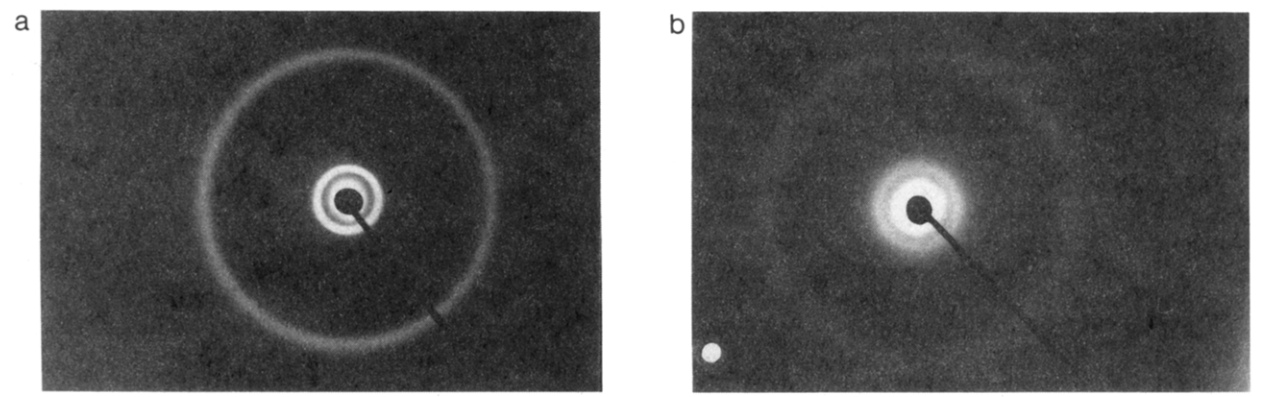

Figure 6. Small-angle X-ray diffraction patterns of (a) sample DB2 and (b) sample DB8 (25 °C).

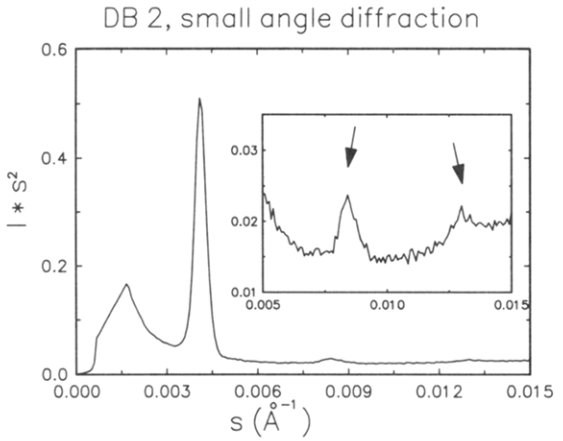

Figure 7. Small-angle X-ray diffractogram of sample DB2 (lamellar morphology).

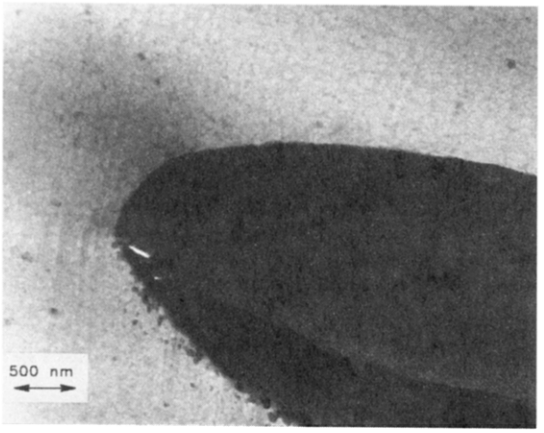

Figure 8. TEM picture of a blend of both homopolymers with volume contents of 50%, respectively, stained with RuO_4 (PS appears dark).

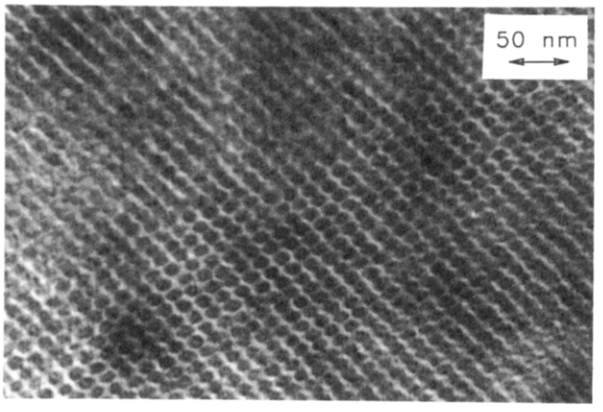

Figure 9. TEM picture of the rodlike morphology of sample DB7 stained with RuO_4 (PS appears dark).

9), and spherical (Figure 11a,b) morphologies have been found as expected. Cylindrical morphologies are only observed in the case of PS rods embedded in a matrix of the LC block (Figure 9). It was not possible to obtain completely uniform areas of orientation, but this was of advantage since views in the rod direction as well as perpendicular to the rods could be recorded simultaneously. Top views of the rods are clearly visible. There is a hexagonal arrangement of the rods is only in small, possibly during the cutting process deformed areas. Larger areas show also a tetragonal arrangement of the rods.[17] This has been observed in the case of the diblock copolymer as well as in the case of the triblock copolymers.[17] With an increase of Φ_{PS} lamellar phases and with a decrease of

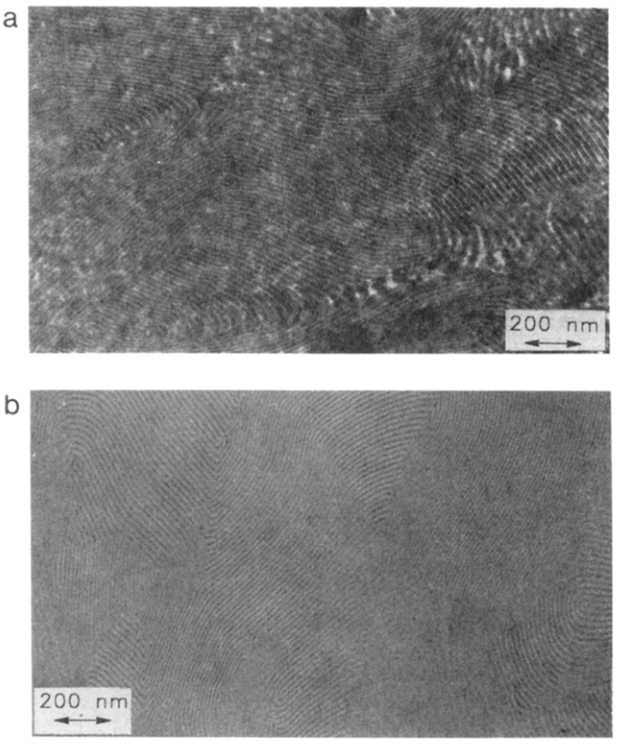

Figure 10. TEM pictures of sample DB11 (lamellar morphology): (a) PS block stained with RuO_4 (appears dark); (b) PChEMA block stained with OsO_4 (appears dark).

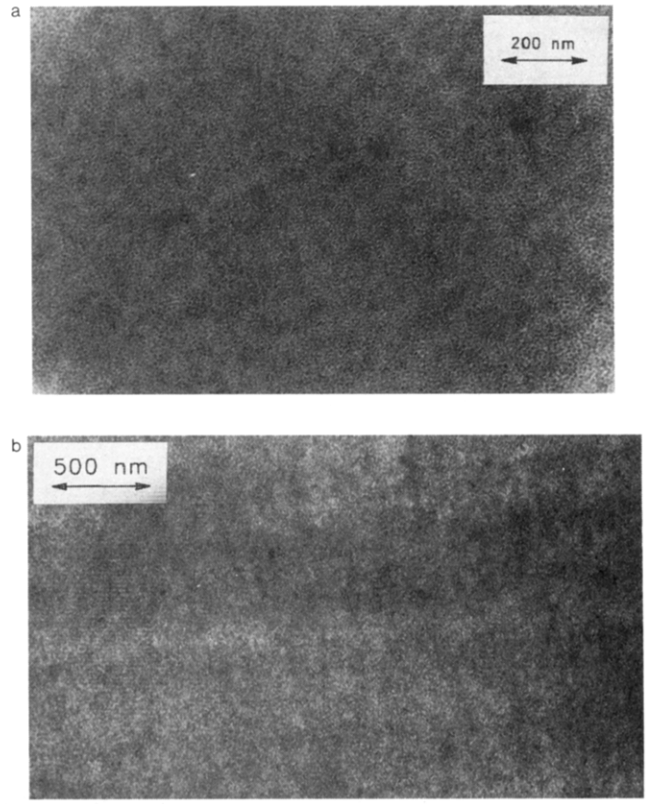

Figure 11. TEM pictures of spherical morphologies: (a) sample 75 (PS block stained with RuO_4, appears dark); (b) sample DB19 (PChEMA block stained with OsO_4, appears dark).

Φ_{PS}, spherical phases are found. To examine block copolymers with smaller Φ_{PS}, a different staining technique was used.[18,19] Figure 10b shows the lamellar phase of DB11, similar to that in Figure 10a. However, in Figure 10a the styrene block was stained and in Figure 10b the methacrylate block was stained. The volume fraction of the

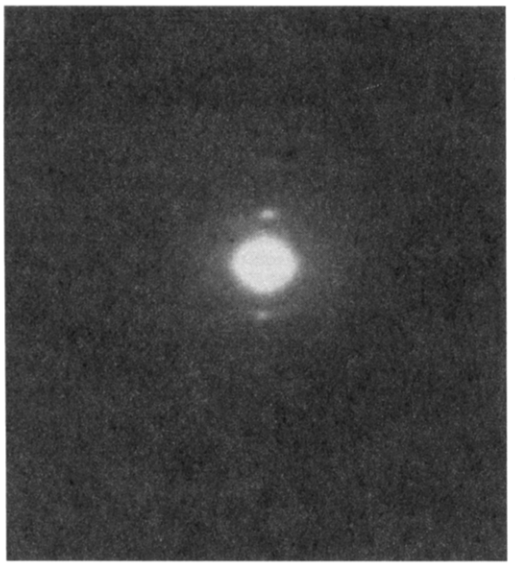

Figure 12. Low-angle electron diffractiion pattern of sample DB11 (lamellar morphology).

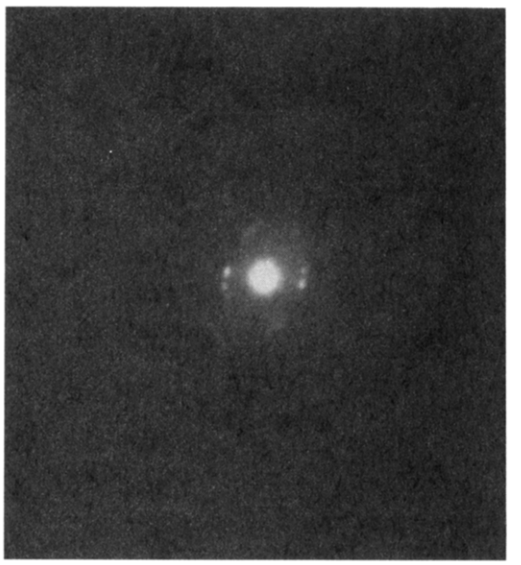

Figure 13. Low-angle electron diffraction pattern of sample DB7 (hexagonal morphology).

methacrylate main chain is comparatively small; therefore, only very small lines are visible. Most of the volume of the phase of the LC block is filled with cholesteryl units. Also with this technique the cylindrical phase of LC-block rods embedded in the PS matrix was not found; only the spherical phase of LC spheres was observed (Figure 11b). The small differences in the observed morphologies compared to ref 13 can be explained by the fact that in ref 13 aligned samples for the SAXS studies have been used. Fibers were drawn from the samples at high temperatures, which might have caused a change in morphology.

To confirm the observed morphologies with diffraction pattern, low-angle electron diffraction studies were carried out, using the procedure described by Bassett and Keller[15] and Kämpf et al.[20] Compared with X-ray diffraction techniques, the advantages of their method are, first, the resolution limit is very much smaller (~4000 Å) in the case of low-angle electron diffraction as stated by Bassett and Keller.[15] Secondly, the exposure time is also smaller than in the case of X-ray diffraction. Also, due to the point focus of the electron beam, two-dimensional resolution is immediately obtained without slit desmearing approximation procedures etc. Finally, the area with a uniform orientation can be much smaller (25 μm^2) compared to the small-angle X-ray diffraction (~1 mm^2). Therefore it was possible to select large areas with a uniform orientation in the transmission mode prior to switching to the diffraction mode. Unfortunately, it is quite difficult to find a suitable calibration standard. Therefore, the diffraction patterns obtained have only qualitative meaning. Figures 12 and 13 show the low-angle electron diffraction patterns of different areas of samples DB11 and DB7 confirming the lamellar and hexagonal morphologies. The orientational relationship between the smectic layers and the microdomain surface will be the subject of a further paper.[21]

Finally, it was possible to draw a phase diagram of the observed morphology dependence on the volume fraction of PS, Φ_{PS} (see Figure 14). It appears that the dividing lines of the areas of spherical morphologies are very well defined due to the fact that on both lines there are two data points of samples showing both morphologies. The open circles represent a nematic structure of the subphase whereas the filled symbols represent the smectic A phase

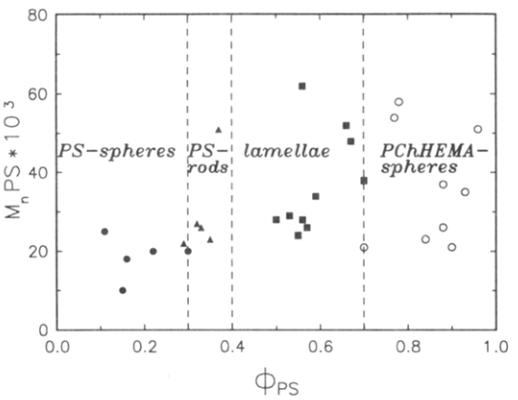

Figure 14. Phase diagram of the observed block copolymers.

of the subphase. As already stated, rods of PChEMA embedded in PS have never been observed. Considering a symmetric phase diagram, the area of the rodlike phase of PChEMA is obviously occupied by the lamellar phase. This is understandable if one takes the structure of the subphase into account. The formation of the thermodynamically stable smectic A phase in the subphase is energetically more favorable than the formation of an equilibrium morphology. On the other hand, the energetic differences between lamellar and rodlike phases are smaller than the differences in energy terms between a nematic and a smectic structure. A smectic phase can only be realized in continuous subphases like lamellar or matrix phases, not in rods or spheres with a very small diameter compared to the layer spacing. The influence of the subphase on the morphology is stronger.

Conclusions

In those samples where the liquid crystalline subphase is not continuous (spheres), only a nematic phase is seen, whereas in all samples in which there is a continuous liquid crystalline subphase, the smectic A phase of the homopolymer is formed. Obviously, there is some influence on the phase structure of the liquid crystalline subphase exerted by the morphological structure. The dimensions of the subphases, being only 200 Å in a spherical subphase, mean that only a few layers of the liquid crystalline structure should be present. This is clearly not enough for a smectic phase to form.

References and Notes

(1) Alward, D. B.; Kinning, D. J.; Thomas, E. L.; Fetters, L. J. *Macromolecules* **1986**, *19*, 215.
(2) Kinning, D. J.; Thomas, E. L.; Alward, D. B.; Fetters, L. J.; Handlin, D. L., Jr. *Macromolecules* **1986**, *19*, 1288.
(3) Thomas, E. L.; Alward, D. B.; Kinning, D. J.; Martin, D. C.; Handlin, D. L., Jr.; Fetters, L. J. *Macromolecules* **1986**, *19*, 2197.
(4) Hasegawa, H.; Tanaka, H.; Yamasaki, K.; Hashimoto, T. *Macromolecules* **1987**, *20*, 1651.
(5) Spontak, R. J.; Smith, S. D.; Ashraf, A. *Macromolecules* **1993**, *26*, 956.
(6) Bates, F. S.; Fredrickson, G. H. *Annu. Rev. Phys. Chem.* **1991**, *41*, 525.
(7) Kodaira, T.; Mori, K. *Makromol. Chem.* **1992**, *193*, 1331.
(8) Heft, M.; Springer, J. *Makromol. Chem., Rapid Commun.* **1990**, *11*, 397.
(9) Blankenhagel, M.; Springer, J. *Makromol. Chem.* **1992**, *193*, 3031.
(10) Bohnert, R.; Finkelmann, H.; Lutz. P. *Makromol. Chem., Rapid Commun.* **1993**, *14*, 139.
(11) Adams, J.; Gronski, W. *Makromol. Chem., Rapid Commun.* **1989**, *10*, 553.
(12) Zaschke, B.; Frank, W.; Fischer, H.; Arnold, M. *Polym. Bull.* **1991**, *27*, 1.
(13) Arnold, M.; Poser, S.; Fischer, H.; Frank, W.; Utschick, H. *Makromol. Chem., Rapid Commun.* **1994**, *15*, 487.
(14) von Mahl, H.; Weitsch, W. *Z. Naturforsch.* **1960**, *A15*, 1051.
(15) Bassett, G. A.; Keller, A. *Philos. Mag.* **1964**, *9*, 817.
(16) Pan, T.; Huang, K.; Balasz, A. C.; Kunz, M. S.; Mayes, A. M.; Russell, T. P. *Macromolecules* **1993**, *26*, 2860.
(17) Fischer, H. *Polym. Commun.* **1994**, *35*, 3286.
(18) Kanig, C.; Neff, H. *Colloid Polym. Sci.* **1975**, *253*, 29.
(19) Misra, S. C.; Pichot, G.; El-Asser, M. S.; Vanderhoff, J. W. *J. Polym. Sci., Polym. Lett. Ed.* **1979**, *17*, 562.
(20) Kämpf, G.; Krömer, H.; Hoffmann, M. *J. Macromol. Sci., Phys.* **1972**, *B6*, 167.
(21) Fischer, H.; Poser, S.; Arnold, M. *Liq. Cryst.*, accepted for publication.